Published OnlineFirst January 15, 2020; DOI: 10.1158/1535-7163.MCT-19-0928

Extracellular Vesicle–Mediated *In Vitro* Transcribed mRNA Delivery for Treatment of HER2$^+$ Breast Cancer Xenografts in Mice by Prodrug CB1954 without General Toxicity

Alexis V. Forterre[1], Jing-Hung Wang[1], Alain Delcayre[2], Kyuri Kim[3], Carol Green[3], Mark D. Pegram[4], Stefanie S. Jeffrey[5], and A.C. Matin[1]

ABSTRACT

Prodrugs are harmless until activated by a bacterial or viral gene product; they constitute the basis of gene-delivered prodrug therapies called GDEPT, which can kill tumors without major side effects. Previously, we utilized the prodrug CNOB ($C_{16}H_7ClN_2O_4$; not clinically tested) and enzyme HChrR6 in GDEPT to generate the drug MCHB ($C_{16}H_9ClN_2O_2$) in tumors. Extracellular vesicles (EVs) were used for directed gene delivery and HChrR6 mRNA as gene. Here, the clinical transfer of this approach is enhanced by: (i) use of CB1954 (tretazicar) for which safe human dose is established; HChrR6 can activate this prodrug. (ii) EVs delivered *in vitro* transcribed (IVT) HChrR6 mRNA, eliminating the potentially harmful plasmid transfection of EV producer cells we utilized previously; this has not been done before. IVT mRNA loading of EVs required several steps. Naked mRNA being unstable, we ensured its prodrug activating functionality at each step. This was not possible using tretazicar itself; we relied instead on HChrR6's ability to convert CNOB into MCHB, whose fluorescence is easily visualizable. HChrR6 mRNA-translated product's ability to generate fluorescence from CNOB vicariously indicated its competence for tretazicar activation. (iii) Systemic IVT mRNA–loaded EVs displaying an anti-HER2 single-chain variable fragment ("IVT EXO-DEPTs") and tretazicar caused growth arrest of human HER2$^+$ breast cancer xenografts in athymic mice. As this occurred without injury to other tissues, absence of off-target mRNA delivery is strongly indicated. Many cancer sites are not amenable for direct gene injection, but current GDEPTs require this. In circumventing this need, a major advance in GDEPT applicability has been accomplished.

Introduction

We recently described our initial attempts (1) at developing targeted gene-delivered enzyme prodrug therapy (GDEPT) to treat HER2$^+$ breast cancer, which remains a serious disease. While antibody-based therapeutics and kinase inhibitors targeting the HER2 receptor are effective (2–4), 10-year follow-up studies show drug-resistant relapse in $\geq$25% in early-stage treated patients (5). Prodrugs are harmless in their native state but are converted into toxic drugs when activated by an enzyme of bacterial or viral origin (6–8). Confining the enzyme-encoding gene to the tumor will localize toxicity to the cancer abating the side effects of conventional chemotherapy. Current GDEPTs are not targeted and require gene injection in cancer site, limiting their usefulness: many cancers, especially multiple sites of metastatic cancer, are not amenable to direct gene injection. Our goal is a regimen for gene delivery specifically to cancer upon systemic administration.

Our previous approach (1) had several innovative features: (i) use of extracellular vesicles ("EVs; also called exosomes; ref. 9), generated by Human embryo kidney 293 (HEK293) cells, for gene delivery; these EVs are nontoxic in mice (1, 10). EV-mediated foreign mRNA delivery had not been accomplished before (Discussion). EVs are 30–100 nm lipid bilayers generated by body cells, performing intercellular exchange of biomolecules believed to be physiologically important (11). Being natural antigen carriers, they may be less immunogenic than viruses and nanoparticles. That they can avoid the lysosomal–endosomal pathway and phagocytosis effectively enough for targeted delivery of si- and miRNAs is well established (refs. 12, 13; Discussion).

(ii) We used mRNA instead of DNA for gene delivery. mRNA is translated directly upon cytosol entry, resulting in efficient gene expression; in contrast, DNA transcription has to precede translation, requiring nucleus entry, which is highly inefficient (<0.10% of cytosolic DNA enters the nucleus; ref. 14). mRNA does not pose the danger of insertional mutagenesis, and mRNA, unlike DNA, is translated in dormant cells (14), which are present in tumors (15). mRNA-based gene delivery has had limited application, but the available comparisons with DNA indicate its superiority (16).

(iii) Our regimen consisted of a new prodrug CNOB ($C_{16}H_7ClN_2O_4$) that we discovered, and our bacterial enzyme, HChrR6, which we have improved and humanized. HChrR6 reductively activates CNOB (17) into the toxic drug MCHB ($C_{16}H_9ClN_2O_2$), which can kill several cancer cell types by apoptosis. MCHB is strongly fluorescent and can be quantitatively imaged in living mice; this greatly facilitated the development of HChrR6/CNOB therapy (17, 18).

(iv) Loading of exogenous functional mRNA into the EVs has been problematic; we accomplished this by constructing a novel plasmid (1).

(v) We designed a novel chimeric construct, called the "extracellular-vesicle-HER2-binding (EVHB)" protein; it contains a high

[1]Department of Microbiology and Immunology, Stanford University School of Medicine, Stanford, California. [2]ExoThera LLC, Menlo Park, California. [3]SRI International, Menlo Park, California. [4]Department of Medicine, Stanford University School of Medicine, Stanford, California. [5]Department of Surgery, Stanford University School of Medicine, Stanford, California.

Note: Supplementary data for this article are available at Molecular Cancer Therapeutics Online (http://mct.aacrjournals.org/).

Corresponding Author: A.C. Matin, Stanford University School of Medicine, 299 Campus Drive West, Stanford, CA 94305-5124. Phone: 650-725-4745; Fax: 650-725-6757; E-mail: a.matin@stanford.edu

Mol Cancer Ther 2020;19:858–67

doi: 10.1158/1535-7163.MCT-19-0928

Published OnlineFirst January 15, 2020; DOI: 10.1158/1535-7163.MCT-19-0928

affinity anti-HER2 single-chain variable fragment [scFv; $K_d = 10^{-9}$ mol/L] and attaches to the EV surface by its lactadherin C1-C2 domains, targeting them to the HER2 receptor. These HChrR6 mRNA–loaded and -targeted EVs are termed "P EXO-DEPTs;" "P" indicates that the mRNA loading involved a plasmid. For ease of reference, schematics of the EVHB protein and the P EXO-DEPTs are reproduced as Supplementary Fig. S1 (1).

In vitro, the P EXO-DEPTs delivered functional HChrR6 mRNA to $HER2^+$ but not to $HER2^-$ cells, and when administered systemically along with CNOB, they arrested the growth of $HER2^+$ human breast cancer xenografts in athymic mice (1), showing that they delivered the HChrR6 mRNA to the xenografts. But how specific was this delivery to the xenografts was not investigated.

This aspect is explored here. Also, we have made changes to our previous regimen to enhance its clinical transfer prospects: use of the prodrug, CB1954 (tretazicar) which, unlike CNOB, has been in clinical trial with its safe human dose published previously (6, 7); and delivery by targeted EVs of *in vitro* transcribed (IVT) HChrR6 mRNA instead of mRNA inserted using a plasmid; plasmids can have harmful effects.

IVT mRNA loading of EVs required several steps (**Fig. 1**). Naked mRNA being unstable, we ensured its prodrug activating functionality during these steps. This was not possible with CB1954 (see below); we relied instead on HChrR6's ability to convert CNOB into MCHB, whose fluorescence is easily visualizable. HChrR6 mRNA-translated product's ability to generate fluorescence from CNOB (the "MCHB test;" see below) vicariously indicated its competence for CB1954 activation.

We show that systemic IVT mRNA–loaded EVs displaying ML39 scFv ("IVT EXO-DEPTs") and tretazicar caused near-complete growth arrest of human $HER2^+$ breast cancer xenografts in athymic mice at a lower EV dose than before (1). As this occurred without injury to other tissues, absence of off-target mRNA delivery is strongly indicated. Many cancer sites are not amenable for direct gene injection, but current GDEPTs require this. In circumventing this necessity, a major advance in GDEPT applicability has been accomplished.

Materials and Methods

Cell lines and viability

HEK293 and the $HER2^+$ human breast cancer BT474 cell lines have been described previously (1). They were purchased from ATCC between 2005 and 2009 and authenticated (December 2017; Genetic Resources Core Facility, Johns Hopkins University, Baltimore, MD). Experiments were done within 1-year of the *Mycoplasma* test (Look-Out Mycoplasma PCR Detection; Sigma-Aldrich; and PCR based MycoDetect kits; Greiner Bio-One North America) showing negativity. Cells were cultured (moisturized incubator, 37°C, 5% CO_2) in DMEM (Thermo Fisher Scientific) 10% FBS and used within 20 passages; MTT Assay (Roche) determined viability.

EV preparation

As before (1, 19), 5×10^6 HEK293 "producer" cells [in 10 mL DMEM, plus 10% EV-depleted FBS ("DMEM-EDFBS")] were plated in a 100-mm dish (4-day incubation). Cells and apoptotic bodies were removed (centrifugation, 600 and 2,000 × *g*, respectively, 30 minutes). The supernatant was centrifuged (100,000 × *g*, 75 minutes); pelleted EVs were suspended in PBS. Bradford Assay quantified protein. The resulting EVs conformed the MISEV standard (9): uniform peak (NanoSight) and average size of approximately 100 nm [NanoSight and transmission electron microscopy (TEM)]; positive for EV-specific proteins: CD63, CD81, and lactadherin (1).

Construction of the EVHB protein

The EVHB protein binds EVs by its C1-C2 domains, making them target $HER2^+$ cells because of its anti-HER2 scFv (Supplementary Fig. S1). As before, the anti-HER2 ML39 scFv DNA sequence (from pACgp67B-HER2m; Addgene) was inserted into p6mLSC1C2 (1) to construct pEVC1C2HER. The producer HEK293 cells, transfected with this plasmid, generated EVs displaying EVHB, which was purified as before (1).

Loading EVs with HChrR6 mRNA and construction of IVT EXO-DEPTs

Loading functional exogenous mRNA into the EVs proved difficult (see below). We previously accomplished this by constructing a new plasmid termed, pXPort/*HChrR6* mRNA, using the System Biosciences XPort plasmid and the zipcode sequences (20) inserted at the 3′-untranslated region of the HChrR6 gene (MSCV promoter). pXPort/*HChrR6* mRNA-transfected HEK293 cells generated HChrR6 mRNA-containing EVs (1).

Here, we succeeded, to our knowledge for the first time, in loading EVs with functional IVT mRNA (Results). These were converted into IVT EXO-DEPTs, as before (Supplementary Fig. S1): 2×10^7 EVs were incubated with pure EVHB (1 μg, room temperature, 15 minutes). NanoSight (NS300; Melvin Instruments), and TEM (JEOL JEM1400) analyses showed that they fully resembled P EXO-DEPTs (Supplementary Fig. S2; ref. 1), conforming to the MISEV standard (9).

MCHB test

This test was used to vicariously determine the capability of translated HChrR6 mRNA to activate tretazicar (which was not practical using tretazicar itself; Results). HChrR6 enzyme (previously named ChrR21) can also reductively activate tretazicar: when tretazicar (15 μmol/L) was incubated with HChrR6 (10 μg/mL, 37°C), it killed >80% breast cancer cells (24-hour incubation, $P > 0.01$; ref. 21). In the MCHB test, IVT HChrR6 mRNA was tested for generating MCHB fluorescence upon CNOB addition in a standard reaction mixture; this contained translated HChrR6 protein + CNOB (15 μmol/L) + NADPH (1 mmol/L; refs. 17, 22). MCHB fluorescence was measured in SpectraMax Plate Reader (Molecular Devices; excitation, 570 nm; emission, 620 nm). Generation of fluorescence from CNOB vicariously indicated the enzyme's competence for tretazicar activation.

HChrR6 mRNA transcription, translation, and enzyme assay *in vitro*

To generate IVT mRNA, the *HChrR6* gene was extracted from puC57-HChrR6, using KpnI (1, 17, 22) and was cloned into pcDNA6/myc-HisA (Thermo Fisher Scientific); in-frame insertion was confirmed (Stanford University Protein and Nucleic Acid Facility). pcDNA6/myc-HisA-SHChrR6 was used to transcribe HChrR6 mRNA *in vitro* (HiScribe T7 ARCA mRNA Kit with tailing; New England Biolabs). mRNA was quantified (NanoDrop 1000 Spectrophotometer; Thermo Fisher Scientific) and used to synthesize cDNA (M-MuLV reverse transcriptase, New England Biolabs); RNaseH treatment (New England Biolabs) removed any remaining mRNA. Quantitative reverse transcription-PCR (qRT-PCR) employed Maxima SYBRGreen/ROX qPCR Master Mix Kit (Thermo Fisher Scientific) and 7500/7500 Fast Real-Time PCR System (Applied Biosystems); GAPDH mRNA served as endogenous control.

The primers employed for HChrR6 and GAPDH have been specified before (1). mRNA amount estimation employed a standard curve relating C_t value with mRNA quantity. EV mRNA copy number

Published OnlineFirst January 15, 2020; DOI: 10.1158/1535-7163.MCT-19-0928

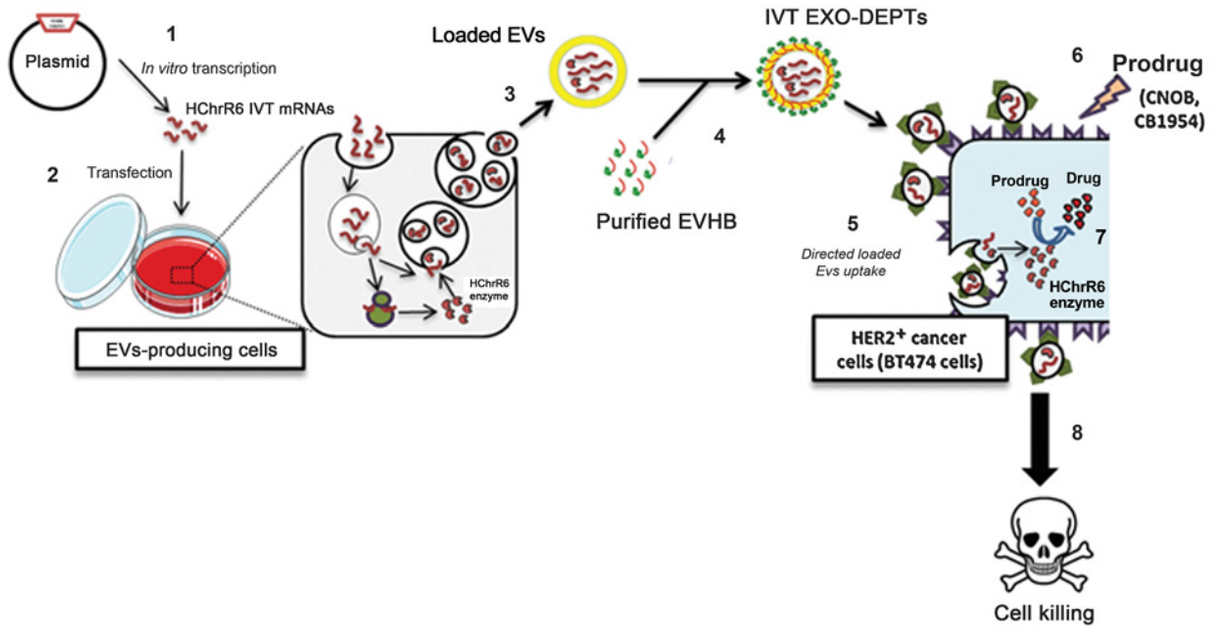

Figure 1.

Schematic of IVT EXO-DEPT preparation and use, involving several steps. (1) Generation of IVT HChrR6 mRNA. (2) Its transfection into HEK293 cells in the presence of polyethylenimine. (3) Confirmation that EVs generated by loaded HEK293 producer cells contain HChrR6 mRNA. (4) Conversion of loaded EVs into IVT EXO-DEPTs by incubation with purified EVHB protein. (5) IVT EXO-DEPT–mediated delivery of HChrR6 mRNA to BT474 cells. (6) Addition of the prodrug CNOB or CB1954 (tretazicar). (7) Prodrug conversion within the cells into the drug. (8) Cell death.

calculation was by the formula: [X (ng) $\times$ 6.0221 $\times$ 10^{23} (molecules/mole)]/[$N \times 330$ (g/mole) $\times$ 10^{9} (ng/g)], where X is the amount of EV mRNA, N is its length, and 330 is the average molecular weight of individual nucleotides (Rhode Island Genomics and Sequencing Center).

IVT mRNA was translated *in vitro* (PURExpress Kit, New England Biolabs); the resulting HChrR6 protein was MCHB test positive. *E. coli* dihydrofolate reductase (DHFR Control Template) supplied in the kit was used to ensure correct translation; it was MCHB test negative, serving as negative control for the translated HChrR6 mRNA.

Loading of EVs with IVT HChrR6 mRNA

The EV-depleted fresh medium (DMEM-EDFBS) was prepared as before (ultracentrifugation; 110,000 $\times$ g; 4°C; ref. 1). HEK293 cells (7 $\times$ 10^{5}) seeded in 6-well plates were transfected with HChrR6 IVT mRNA (2 μg/well) using Polyethyleneimine (PEI, 2.5 $\times$ mRNA), unbound PEI was removed, the medium replaced (24 hours later) with fresh EV-depleted medium, incubated (37°C, 4 days), and the EVs were isolated. Total RNA extraction from the producer cells and the EVs employed RNeasy Mini Kit (Qiagen); HChrR6 mRNA was quantified as above.

Flow cytometry

IVT EXO-DEPTs (**Fig. 3** legend provides numbers) were stained with PKH26 dye (4 μL in 1 mL Diluent C; Sigma-Aldrich; ref. 1), washed twice to remove unbound dye, and quantified for protein. They were incubated with BT474 cells (3 wells of a 6-well plate), washed (PBS), dislodged (trypsin), suspended in DMEM/10% FBS, harvested (900 $\times$ g; 4°C; 5 minutes), washed with 1 mL of acid buffer (0.5 mol/L NaCl; 0.2 mol/L acetic acid, pH 3.0) to remove non-internalized EVs, and treated with Flow Cytometry Fixation Buffer (R&D Systems; 4°C; overnight). The cells were pelleted (900 $\times$ g; 4°C; 5 minutes), resuspended in 1 mL FACS buffer (PBS/1% BSA/0.1% NaN_3), and analyzed at the Scanford FACS Analyzer (excitation, 488 nm; emission, 590/20 nm).

In vitro assays

To test functionality of the translated HChrR6 mRNA, different amounts of it (Results) were subjected to the MCHB test. HChrR6 mRNA in IVT- and P EXO-DEPTs was quantified as above. For comparison of their efficacy in donating HChrR6 mRNA, BT474 cells (see **Fig. 4** legend for numbers) were incubated (DMEM-EDFBS; 100 μL in a 96-well plate; 37°C; 5% $C0_2$) with IVT- or P EXO-DEPTs (or with directed unloaded "control" EVs; ref. 1). Incubation medium was replaced with fresh DMEM-EDFBS containing 15 μmol/L CNOB. After incubation (Results), the exposed cells were subjected to the MCHB test by measuring MCHB fluorescence.

In vivo assay of IVT EXO-DEPT functionality

Animal experiments were approved by Stanford University Institutional Animal Care and Use Committee. As before (1), the number of mice was determined using the G*Power calculator (Universitat Dusseldorf) for F-tests of one-way ANOVA by setting Type I error at 5% (alpha = 0.05); power was kept at 0.8, and the number of treatment groups, 4. The effect size, f, was calculated as 0.707 and indicated total sample size of 28 with 7 mice per treatment group. Five- to 6-week-old female BALB/C athymic nude mice (Charles River Laboratories) were implanted subcutaneously with 17β-estradiol pellets (Innovative Research of America) to support growth of xenografts of BT474 (estrogen positive) cells. A total of 10^{7} cells were injected subcutaneously. For full details of the procedure, see (1). Caliper was used to measure tumor size at 2-day intervals. Tumor volume and

Published OnlineFirst January 15, 2020; DOI: 10.1158/1535-7163.MCT-19-0928

growth rate were calculated using the formula: tumor width^2 × its length/2, and from slopes of linear regression, respectively. When the tumors reached a volume of approximately 180 mm^3, the mice were assigned to four groups and treatments started (Results).

Toxicology and histopathology

Following mice euthanasia, serum and whole blood were collected. Organs (spleen, kidney, liver, heart, lung, and brain) were harvested and fixed in 10% neutral buffered formalin to perform toxicology and histopathology analyses; these were conducted at SRI Biosciences. The tissues were processed by routine methods, sectioned, mounted on slides, and stained with hematoxylin and eosin.

Data and statistical analysis

Excel2010 software was used. Statistics were determined using Student t test; $P < 0.05$ was considered significant.

Results

Rationale of the MCHB test

Making IVT EXO-DEPTs and their use involved multiple steps, for example, IVT mRNA synthesis, its loading into HEK293 cells, isolating mRNA-loaded EVs, and others illustrated in **Fig. 1**. As naked mRNA can be highly unstable (refs. 23, 24; Discussion), it was necessary to ascertain that the translated HChrR6 mRNA remained tretazicar activation–competent during these steps. The drug generated by tretazicar reduction is (5-(aziridine-1-yl)-4N-acetoxy-2-nitrobenzamide (referred to from here on as "nitrobenzamide"). Reliable detection of nitrobenzamide requires complex high-performance liquid chromatography–based methods (25), which was impractical, given the multiplicity of steps (**Fig. 1**). However, the fact that HChrR6 can activate both CNOB and tretazicar (21) suggested a facile alternative, namely the MCHB test. This was based on the hypothesis that if the translated HChrR6 mRNA could generate MCHB fluorescence upon CNOB addition, it would be capable of activating tretazicar as well; MCHB is strongly fluorescent and thus easily observable. This hypothesis proved correct.

IVT mRNA in EVs

IVT HChrR6 mRNA was synthesized; the MCHB test–based confirmation of its functionality is shown in **Fig. 2A**: increasing amounts of the translated mRNA generated increasing fluorescence upon CNOB addition. HEK293 cells were transfected with this IVT mRNA; qRT-PCR revealed that the EVs generated by these cells contained approximately 3.3×10^{-2} copy of the mRNA/EV. Two copies of the 25-nucleotide "zipcode" sequence promotes mRNA-loading into the EVs (20). However, addition of these to the IVT mRNA did not enhance the loading; so, IVT mRNA without the zipcode was used. As the previously made P EXO-DEPTs (1) contained 2×10^{-4} copy/EV, the IVT method proved an advance, decreasing the number of EVs required to donate one mRNA copy from 5,000 to <50 (**Fig. 2B**).

Was the HChrR6 mRNA in the EVs adhered to their surface? To investigate this, the loaded EVs were incubated with or without RNaseA, followed by mRNA extraction and quantification. No difference resulted from RNase treatment (Supplementary Fig S3); thus, the mRNA was mainly inside the EVs. These IVT EVs were converted into EXO-DEPTs capable to target HER2$^+$ cells by incubation with the EVHB (Supplementary Fig. S1; ref. 1; Materials and Methods).

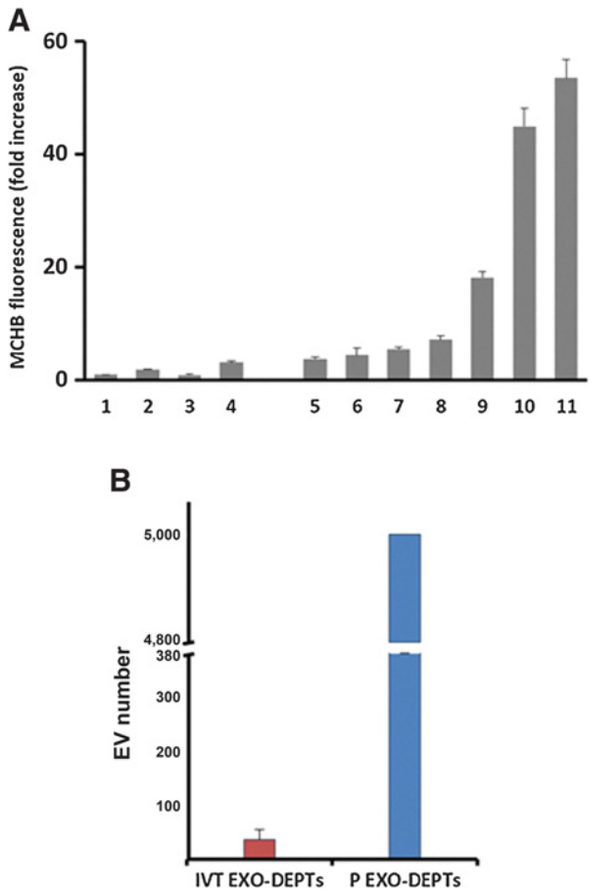

Figure 2.

IVT HChrR6 mRNA functionality and its amount in IVT EXO-DEPTs. **A,** Test of the functionality of IVT HChrR6 mRNA. Its translated product converts CNOB into MCHB as measured from MCHB fluorescence. Increasing amounts of the translated HChrR6 mRNA protein (quantified by Bradford assay) generated increasing fluorescence ($n = 3$). Numbers in the abscissa denote: 1, PBS; 2, CNOB 15 μmol/L; 3, NADPH 1 mmol/L; 4, full reaction mix (Rx) without HChrR6 protein. (CNOB was 15 μmol/L; NADPH, 1 mmol/L); 5, Rx + 2.5 ng protein; 6, Rx + 5 ng protein; 7, Rx + 10 ng protein; 8, Rx + 20 ng protein; 9, Rx + 40 ng protein; 10, Rx + 80 ng protein; and 11, Rx + 160 ng protein. **B,** The IVT EXO-DEPTs contain more HChrR6 mRNA compared with P EXO-DEPTs: <50 of the former (red bar), but 5,000 of the latter (blue bar) are needed to donate one mRNA copy ($n = 3$).

Binding of IVT EXO-DEPTs to cells and their mRNA delivery efficacy

FACS analysis of (PKH26-labeled) IVT EXO-DEPT binding to BT474 cells showed 0.6% attachment at 6-hour incubation, which increased to 80% at 24 hours (**Fig. 3A**). 0.6% attachment roughly corresponds to the exposure of each BT474 cell to some 10 HChrR6 mRNA copies. Quantification of the mRNA delivered by the EVs into the cells can be only approximate due to its degradation, etc. in the recipient cells. To get a rough estimation, total RNA was extracted from the cells at the 6-hour incubation point, and the HChrR6 mRNA copies were measured (qRT-PCR); some five copies of HChrR6 mRNA were detected per recipient cell, suggesting a high transfection ratio; there was no HChrR6 mRNA in cells treated with directed EVs devoid of mRNA (**Fig. 3B**). We suspect that the efficient mRNA delivery by the EVs to the cells is related to their

Published OnlineFirst January 15, 2020; DOI: 10.1158/1535-7163.MCT-19-0928

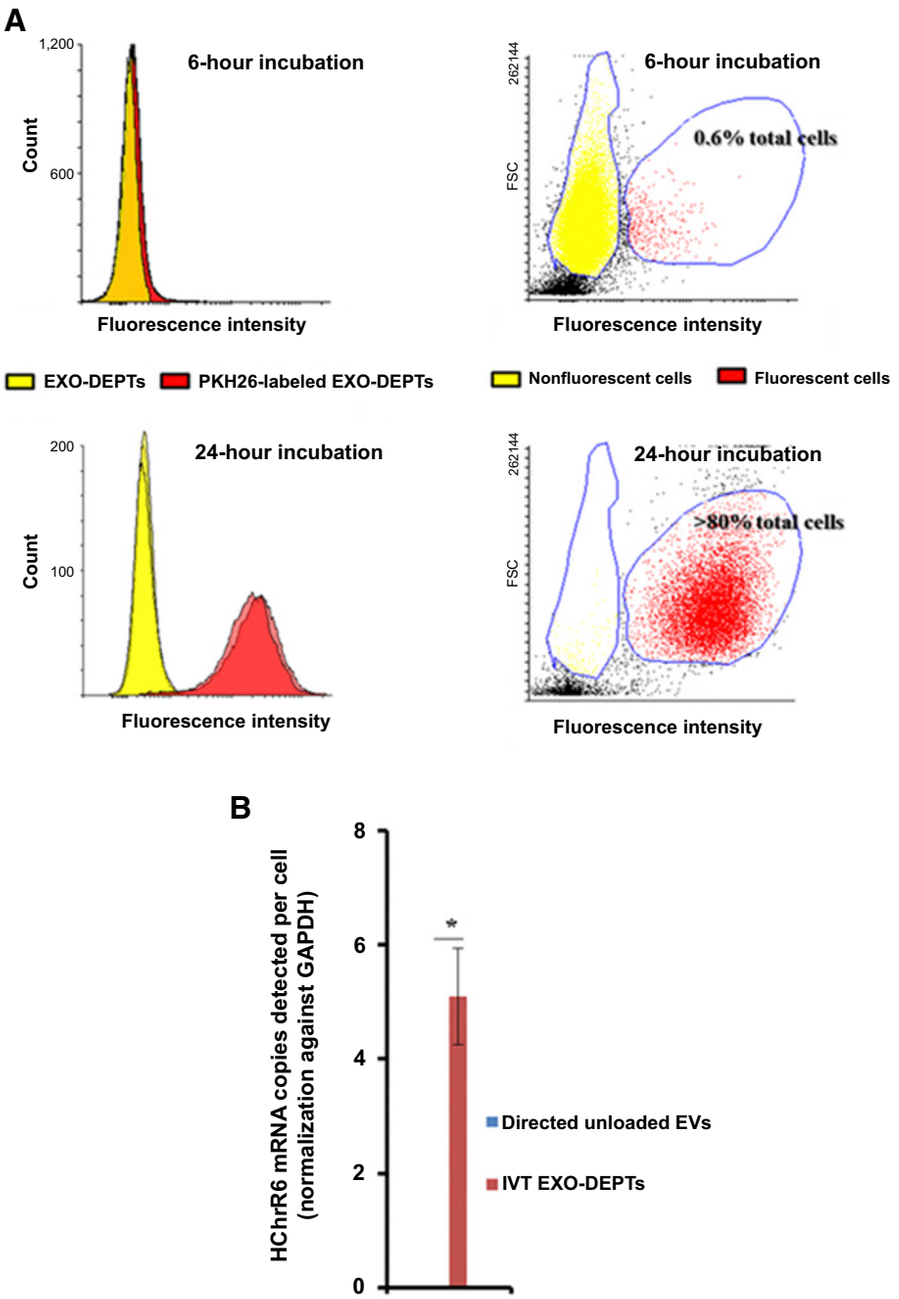

Figure 3.

A, IVT EXO-DEPTs interaction with HER2$^+$ BT474 cells and HChrR6 mRNA delivery. Flow cytometry results of 1.62×10^6 BT474 cells incubated for 6 hours (top), or 24 hours (bottom) with PKH26-labeled (red) or unlabeled (yellow) 5×10^{10} IVT EXO-DEPTs. At 6 hours, 0.6% cells bounded the EVs (red; top, right); at 24 hours this number increases to 80% (bottom, right; $n = 3$). **B,** HChrR6 mRNA copy number in BT474 cells after 6-hour incubation with IVT EXO-DEPTs (red bar). No HChrR6 mRNA was detected in BT474 cells incubated for the same duration with directed EVs not containing the IVT mRNA (*, $P < 0.05$; $n = 3$); consequently, no blue bar (representing unloaded EVs) is seen in the figure.

display of the high affinity [$K_d = 10^{-9}$ mol/L] anti-HER2-scFv that promoted efficient attachment and content release.

EXO-DEPT efficacy *in vitro*

We compared the efficacy of IVT EXO-DEPTs with P EXO-DEPTs in conferring prodrug activating capability on the recipient BT474 cells. Separate batches of the cells were incubated with each kind; numbers were adjusted to deliver the same mRNA copies per recipient cell (see legend to **Fig. 4**); and gene expression was determined by the MCHB test. It increased with time and, except for the first 24 hours, the IVT EXO-DEPT–treated cells showed greater expression during the 120-hour experiment. While the P EXO-DEPT–mediated expression peaked at 72 hours, it continued to increase during the entire experiment with the IVT EXO-DEPTs. Thus, translation of the mRNA donated by the IVT EXO-DEPTs was more efficient and more durable. Cells incubated with control EVs (directed but without HChrR6 mRNA) were MCHB test negative.

For EVs to deliver mRNA to BT474 cells, they needed to be directed. This was shown in our previous study: mRNA loaded but nondirected EVs failed to confer prodrug activating capability on BT474 cells; loaded and directed ones did (ref. 1; **Figs. 3A** and **4C**).

Published OnlineFirst January 15, 2020; DOI: 10.1158/1535-7163.MCT-19-0928

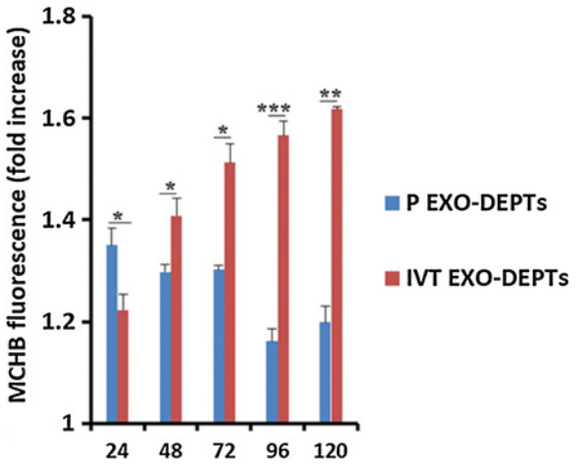

Figure 4.

Comparative efficacy of IVT- and P EXO-DEPTs. Comparison of the kinetics of *HChrR6* gene expression by BT474 cells (10^4) receiving the HChrR6 mRNA by IVT EXO-DEPTs (red bars) or by P EXO-DEPTs (blue bars), as determined by the MCHB test. The number of the two kinds of the EVs was adjusted to deliver 10^4 mRNA copies. This required 3×10^5 IVT- and 5×10^7 P EXO-DEPTs (*, $P < 0.05$; **, $P < 0.01$; ***, $P < 0.001$; $n = 3$). The IVT EXO-DEPTs generate superior results.

Treatment of implanted human HER2$^+$ orthotopic breast cancer xenografts in athymic mice by IVT EXO-DEPTs + tretazicar

As HChrR6 enzyme effectively activates both CNOB and tretazicar (21), we followed our previous protocol, which achieved near-complete growth arrest of xenografts in mice (1): the EVs were administered in two doses and tretazicar in six (**Fig. 5A**). As before, we administered a total of 2.8×10^7 mRNA copies/mouse. Because the IVT EXO-DEPTs had more HChrR6 mRNA, fewer of these were needed, 6.8×10^8 instead of 1.5×10^{11} needed for the P EXO-DEPTs (1). Each test group consisted of 7 mice. Treatments began after the mice developed measurable (180 mm^3) tumors. In mice receiving no treatment, there was vigorous tumor growth, reaching a volume of 400–450 mm^3 and growth rate of 5 mm^3/day (**Fig. 5B** and **C**). But in mice receiving both the IVT EXO-DEPTs and tretazicar (CB1954; "full treatment"), the xenograft growth was minimal and stopped by day 8. The last EV and tretazicar doses were given on days 4 and 7, respectively (**Fig. 5A**), showing that the tumor growth arrest continued for 21 more days without further treatment. Control mice receiving CB1954 alone exhibited tumor growth resembling the untreated mice.

Tumor targeting specificity can result from enhanced permeability retention effect resulting from blood vessel fenestration in tumors and their impaired lymphatic drainage. Whether this applied to EVs and if so, did the scFv-based targeting strategy we used, conferred any advantage was investigated in our previous study (1). This was done by comparing the effect of administering the prodrug with mRNA-loaded nondirected or directed EVs in separate groups of mice. There was significant arrest of xenograft growth with the former (loaded, nondirected), but the growth arrest was 50% more pronounced when the directed EVs were used (ref. 1; **Fig. 4F**: compare green and blue curves). The result bolstered the suitability both of EVs as targeting vehicles and our scFv-based targeting strategy.

However, whether the anti-Her2 scFv displayed by our EVs by itself retarded tumor growth was not investigated. Current HER2$^+$ breast cancer therapies (e.g., trastuzumab) rely on interfering with HER2-mediated signaling by interacting with the HER2 receptor, and the anti-HER2 scFv of our EVs could have had a similar effect. This was investigated here by injecting mice only with directed EVs not containing HChrR6 mRNA (no prodrug was administered). Their xenograft growth resembled the untreated group (**Fig. 5B** and **C**), indicating that the ML39 scFv played no role in arresting tumor growth and the near-complete growth arrest seen in mice receiving the full treatment was due entirely to prodrug activation. A pilot experiment, in which only two groups of mice were used, untreated and those receiving full treatment ($n = 5$), gave very similar results. Experiments were terminated (day 31), as the tumors in the control groups had begun to exceed the volume allowed by the animal protocol.

Because mRNA delivered by the IVT EXO-DEPTs was expressed for a longer duration than the P EXO-DEPT–delivered mRNA (**Fig. 4**), we wondered whether fewer IVT EXO-DEPTs would also prove effective. The *in vivo* experiment was repeated using either half or one log fewer EVs (1.7×10^8 or 3.4×10^7 EVs, respectively); "full dose" (**Fig. 5**) was used as control. Treatment schedule and the number of mice used for each group were as in **Fig. 5**. The lower doses, however, had no significant effect on the xenograft growth (Supplementary Fig. S4). The reason for this is not known but may be related to the short half-life of EVs in circulation (26), which, at the lower doses, may have decreased the EV number below that required for effective attachment to the xenografts.

Specificity of tretazicar activation in HER2$^+$ xenografts

Because xenograft growth was arrested (**Fig. 5**), it is clear that in the xenografts tretazicar was converted into its cytotoxic product, nitrobenzamide, showing successful delivery of functional HChrR6 mRNA. EVs temporarily colonize pancreas, spleen, and liver (27); furthermore, the ML39 scFv of our EVHB protein might also have recognized mouse ErbbB2–expressing cells. Thus, it was possible that the IVT EXO-DEPTs delivered HChrR6 mRNA also to normal tissues causing them to activate tretazicar, triggering general injury. To investigate this, we performed toxicology and histopathology analyses of mice that received no, or the full treatment, the latter utilized the therapeutic regimen of **Fig. 5** (that resulted in near-complete growth arrest of the xenografts).

The animals were sacrificed at the end of the experiment, and whole blood and serum were collected along with tissues (liver, spleen, kidney, lung, heart, and the brain). **Figure 6** compares results in treated and untreated mice for hematology (A) and serum chemistry (B; abbreviations in the abscissa are standard; see Supplementary Table S1 for full names). The treatment did not significantly affect serum chemistry and whole-blood hematology panels. Changes in platelet counts (PLT), mean platelet volume (MPV), and total neutrophil counts (ANS) were significant ($P < 0.05$). Because these changes were small and affected only three hematologic parameters, no serious bone marrow suppression is indicated.

Four of 7 mice of the treatment group showed minor elevation of liver enzymes aspartate aminotransferase and alanine aminotransferase (**Fig. 6B**); however, the overall group averages were not statistically significant, and this outcome is known to be a transient effect of tretazicar treatment (28). Histopathology evaluations of the tissues, including the liver, showed no difference between treated and untreated mice. Thus, the IVT EXO-DEPT + tretazicar treatment is effective without causing notable off-target injury. We suspect that the high specificity of the anti-HER2 ML39 scFv for human HER2 receptor (29, 30) and the much higher HER2 expression of the breast cancer xenografts compared with the normal tissues account for this result.

Published OnlineFirst January 15, 2020; DOI: 10.1158/1535-7163.MCT-19-0928

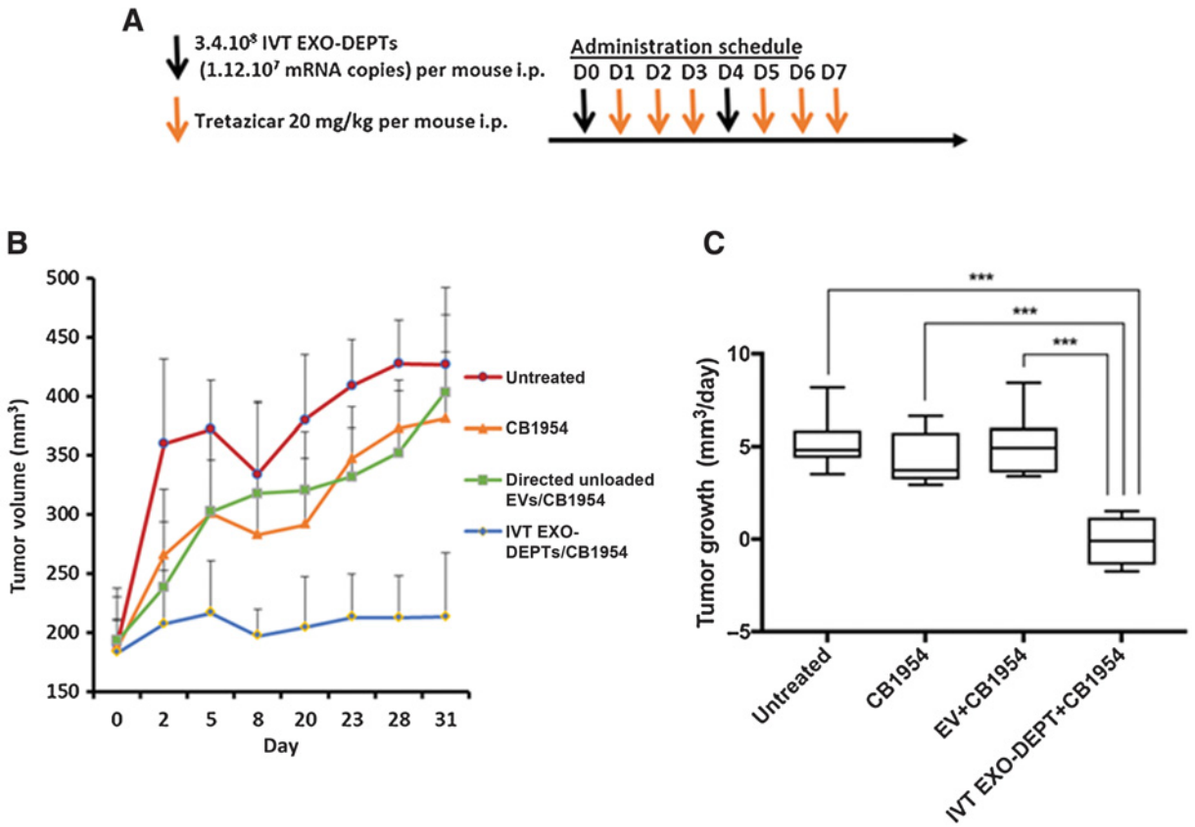

Figure 5.

In vivo effectiveness of the IVT EXO-DEPTs. **A,** Administration schedule; the EXO-DEPT numbers and the tretazicar amount are for each dose per mouse. **B,** Volume of orthotopically implanted BT474 HER2$^+$ xenografts in mice, as measured by a caliper; each data point is mean value for individual treatment groups ($P < 0.001$). The four groups of mice used are identified in the figure. **C,** Box and Whisker plot of the growth rate of the tumors (***, $P < 0.001$; $n = 7$). Mice receiving full treatment (IVT EXO-DEPTs + tretazicar) show near-complete arrest of xenograft growth. i.p. intraperitoneal.

Discussion

Prodrug chemotherapy offers the possibility of confining toxic drug largely to tumors and abating the side effects of most current chemotherapy. Clinical trials of prodrugs have been disappointing (6–8) and the possible reasons for this have been noted. Examples are, problems with gene delivery vehicles, and dearth of: facile methods for detecting prodrug activation (17, 18); of potent activating enzymes (21, 22, 31–33); and of quantification of tumor transfection with the GDEPT gene for generating sufficient bystander effect to kill the whole tumor (17, 18, 34, 35).

Our 2018 article (1) addressed some of these issues. First, use of EVs instead of viruses and nanoparticles for gene delivery. That EVs might be superior is widely recognized, as shown in numerous studies involving si- and miRNA delivery. Examples are, let 7ainordertodeliverlet-7a (let7a) to treat breast cancer in mice (36); plasma siRNAs to blood cells for selective gene silencing (37); siRNA to the brain to treat opiate addiction (38); miR-26 to treat liver cancer (39); miR-16–based mimics to treat malignant pleural mesothelioma (40); and use of DNA minicircle for prodrug treatment (41).

Second, because a major problem revealed in prodrug clinical trials is the dearth of sufficient gene transfer and its short-lived expression in the tumor (6–8), we used mRNA instead of DNA for gene delivery, the former being capable of more efficient translation. We believe to be the first to load EVs with functional exogenous mRNA; this was accomplished by constructing a novel plasmid, pXPort/*HChrR6* mRNA (1). Around the same time, Kojima and colleagues (42) may also have succeeded in this. They used plasmids to bind the catalase mRNA to the EV CD63 protein and showed that their producer cell EVs transferred catalase activity to recipient cells. But they did not report catalase activity of the producer cells, or whether catalase expression in the recipient cells was insensitive to the transcription inhibitor, actinomycin D. Thus, the species transported may have been the catalase-encoding plasmid and/or the catalase protein itself, rather than the catalase-encoding mRNA. Earlier attempts at delivering functional mRNA via EVs had uniformly failed. Electroporation did not work (1); in other attempts, we obtained EVs containing a reporter mRNA generated by plasmid-transfected cells, but this mRNA fragmented during its EV-mediated delivery to recipient cells (19); a similar phenomenon was seen by others (43).

The work reported here advances our therapeutic regimen for clinical transfer in significant ways. First, our systemically administered EXO-DEPTs delivered HChrR6 mRNA to xenografts without off-target injury, showing a high degree of xenograft targeting specificity. Specific delivery of the gene to cancer upon systemic administration is critical for GDEPT effectiveness: not all cancers, and especially cancer metastases, are accessible for direct gene injection upon which the current GDEPTs depend. We note that because the

Published OnlineFirst January 15, 2020; DOI: 10.1158/1535-7163.MCT-19-0928

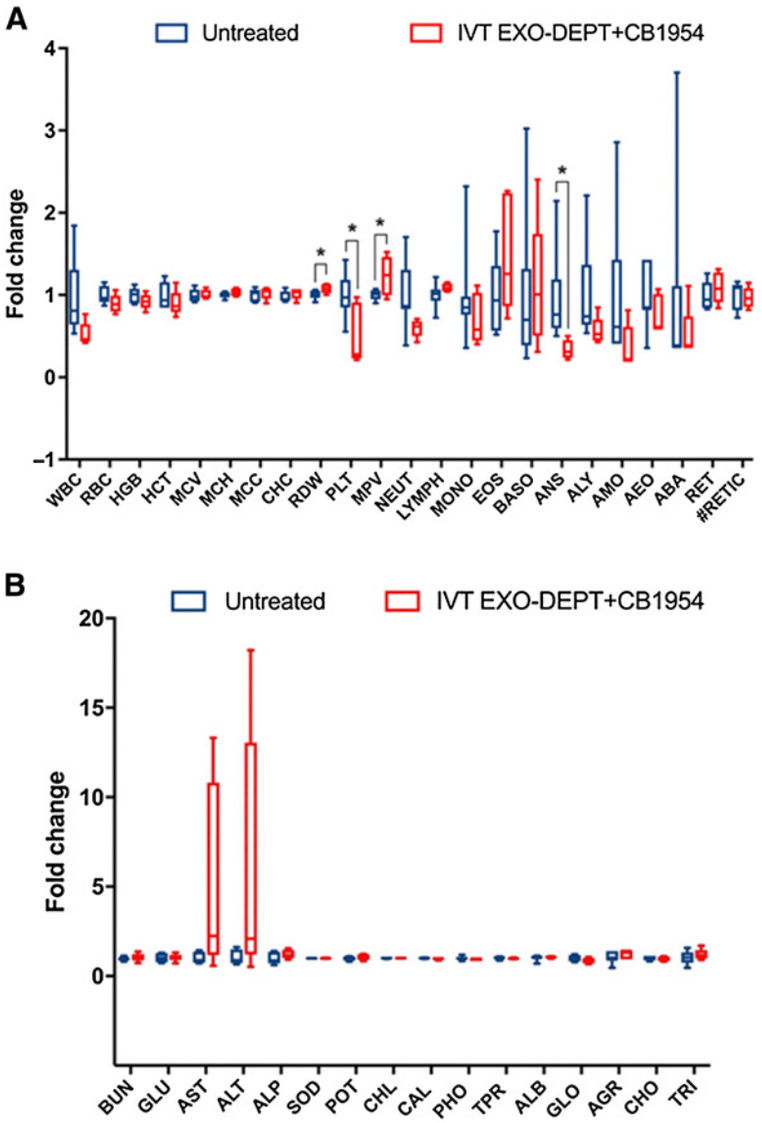

Figure 6.

Hematology and serum chemistry. **A,** Hematology of treated (red) and nontreated (blue) mice. **B,** Serum chemistry of treated and nontreated mice. Abscissa abbreviations for the constituents are standard; they are spelled out in full in Supplementary Table S1, which also provides numerical values. Mice receiving full treatment show essentially no off-target injury.

anti-HER2 scFv in the EVHB protein can be replaced by moieties able to target other receptors, our approach can specifically treat any disease significantly overexpressing a marker. Among cancers alone, the overexpressed receptors include bombastin, folate, and the ligand PSMA as well as others (44–46).

The second element facilitating clinical transfer is the demonstration that our approach can arrest xenograft growth when tretazicar is used as prodrug; this prodrug has been in clinical trials with its safe dose in humans established (6, 7), unlike our previously used prodrug, CNOB (1, 17, 18).

A third seminal element, also to our knowledge accomplished here for the first time, is the loading of the EVs with IVT mRNA avoiding the use of plasmids, which could be harmful to patients. This was a somewhat daunting task because naked mRNA is prone to fragmentation. For example, when introduced into dendritic cells, it was not expressed until transfected in a nanoparticle format; and modifications like the use of RNA patch were needed for effective expression (23, 24, 47, 48). Thus, at each step in this work (**Fig. 1**), we ensured the functionality of our mRNA for prodrug activation. As mentioned, this was impractical using tretazicar itself. But the MCHB test, relying on the HChrR6 enzyme capability to activate both CNOB and tretazicar, and MCHB fluorescence, enabled us to accomplish this.

We constructed IVT EXO-DEPTs for safety reasons, but they afforded additional benefits. They contained greater HChrR6 mRNA copies and were able to arrest xenograft growth with 220-fold fewer EVs than the P EXO-DEPTs used previously (1). The reasons for greater mRNA in the IVT EXO-DEPTs likely are: (i) the IVT mRNA is available directly for transfer into EVs upon entry into the producer cell cytosol; with the pXPort/*HChrR6* plasmid (1) in contrast, the mRNA would become available only after transcription, requiring nucleus entry; (ii) a given amount of genetic material of naked mRNA has an order of magnitude more copies than an equivalent amount of the plasmid encoding it; and (iii) smaller size of mRNA than its encoding plasmid.

The second beneficial IVT EXO-DEPT characteristic is that the mRNA they delivered resulted in more stable gene expression. While the reason for this remains to be determined, it is a salutary outcome in that short-lived gene expression has constrained GDEPT effectiveness (6–8).

Published OnlineFirst January 15, 2020; DOI: 10.1158/1535-7163.MCT-19-0928

Further improvement of our GDEPT is, however, needed. We have so far attained xenograft growth arrest, but successful therapy requires tumor regression and elimination. We posit that recruiting immunity will help achieve this, because HER2$^+$ tumor ablation evokes a strong anti-HER2 immune response (49). We are testing this in immunocompetent FVB/NJ mice, which spontaneously develop HER2$^+$ breast cancer driven by an oncogenic form of human HER2 (HER2Δ16; ref. 50). As stated, HEK 293 EVs we have been using are, by and large, nonimmunogenic, but to further minimize immune rejection, we are using autologous EVs generated by dendritic cells of these mice. Immunogenicity of the human components of the EVHB protein (C1-C2 domains and the anti-HER2 scFv) will, however, remain. While possibly deleterious, it could conceivably be beneficial instead. The lack of general toxicity we report here suggests that the IVT EXO-DEPTs are rapidly attracted to, and may be arrested by, the HER2$^+$ tumor. Thus, the immune rejection may target the tumor and bolster its killing.

Another critical improvement that is needed is to make the IVT EXO-DEPTs more efficient to minimize the need for repeated dosing. Increasing the mRNA content of the EVs and extending its expression in recipient cells can help achieve this. If the IVT mRNA loading of the producer cells can be increased, it is likely that the EVs they generate will also have enhanced content. Available measures for increased mRNA loading of cells include complexation of mRNA with lipofectin (51) and use of a nonlipid cationic reagent, for example, TransMessenger. Stability of mRNA and therefore the likelihood of prolonged expression can be achieved by, for example, the use of β-globin mRNA sequences (52), chemical modifications like replacement of uridine or cytidine by pseudouridine or 5-methylcytidine (53), and reversible addition-fragmentation chain transfer polymerization (54). Moreover, incorporating the TEV start site in the HChrR6 mRNA can strongly enhance its translation (55, 56). Although with some of these measures, care would need to be exercised regarding potential toxicity, there is high probability that suitable methods will be found, given the multiple possibilities noted above and the continuing progress in the field. To conclude, we have taken further important steps for clinical transfer of our regimen, and promising avenues are available to enhance this potential.

Disclosure of Potential Conflicts of Interest

A. Delcayre has ownership interest (including patents) in ExoThera. A.C. Matin has ownership interest (including patents) in Exogene Therapeutics, Inc. No potential conflicts of interest were disclosed by the other authors.

Disclaimer

Stanford University has filed a provisional and foreign patent application encompassing findings in this article (#S17-343 STAN-1442PRV 62/564 and 217 STAN-1442PRV 63/697,758); A.C. Matin, A.V. Forterre, J.-H. Wang, and A. Delcayre, are coinventors. The invention has been provisionally licensed for a possible industry launch, named Exogene Therapeutics, Inc.

Authors' Contributions

Conception and design: A.C. Matin, A.V. Forterre, J.-H. Wang, A. Delcayre, S.S. Jeffrey, M.D. Pegram, C. Green, K. Kim
Development of methodology: A.V. Forterre, J.-H. Wang, K. Kim, C. Green, A.C. Matin, A. Delcayre
Acquisition of data (provided animals, acquired and managed patients, provided facilities, etc.): A.V. Forterre, J.-H. Wang, K. Kim, C. Green, A.C. Matin
Analysis and interpretation of data (e.g., statistical analysis, biostatistics, computational analysis): A.V. Forterre, J.-H. Wang, K. Kim, C. Green, A.C. Matin
Writing, review, and/or revision of the manuscript: A.C. Matin, A.V. Forterre, J.-H. Wang
Administrative, technical, or material support (i.e., reporting or organizing data, constructing databases): A.C. Matin, A.V. Forterre, J.-H. Wang
Study supervision: A.C. Matin

Acknowledgments

Research reported in this article was supported by the National Center for Advancing Translational Sciences of the NIH under Award Number UH3TR000902 to A.C. Matin. JeoL TEM1400 is funded by the NIH Grant SIG number 1S10RR02678001. A.V. Forterre, J.-H. Wang, A.C. Matin, A. Delcayre, K. Kim, C. Green, M.D. Pegram, and S.S. Jeffrey, received support from UH3TR000902.

The costs of publication of this article were defrayed in part by the payment of page charges. This article must therefore be hereby marked *advertisement* in accordance with 18 U.S.C. Section 1734 solely to indicate this fact.

Received September 30, 2019; revised December 2, 2019; accepted January 8, 2020; published first January 15, 2020.

References

1. Wang JH, Forterre AV, Zhao J, Frimannsson DO, Delcayre A, Antes TJ, et al. Anti-HER2 scFv-directed extracellular vesicle-mediated mRNA-based gene delivery inhibits growth of HER2-positive human breast tumor xenografts by prodrug activation. Mol Cancer Ther 2018;17:1133–42.
2. Konecny GE, Pegram MD, Venkatesan N, Finn R, Yang G, Rahmeh M, et al. Activity of the dual kinase inhibitor lapatinib (GW572016) against HER-2-overexpressing and trastuzumab-treated breast cancer cells. Cancer Res 2006;66:1630–9.
3. Slamon D, Eiermann W, Robert N, Pienkowski T, Martin M, Press M, et al. Adjuvant trastuzumab in HER2-positive breast cancer. N Engl J Med 2011;365:1273–83.
4. Yarden Y, Sliwkowski MX. Untangling the ErbB signalling network. Nat Rev Mol Cell Biol 2001;2:127–37.
5. Cameron D, Piccart-Gebhart MJ, Gelber RD, Procter M, Goldhirsch A, de Azambuja E, et al. 11 years' follow-up of trastuzumab after adjuvant chemotherapy in HER2-positive early breast cancer: final analysis of the HERceptin Adjuvant (HERA) trial. Lancet 2017;389:1195–205.
6. Chung-Faye G, Palmer D, Anderson D, Clark J, Downes M, Baddeley J, et al. Virus-directed, enzyme prodrug therapy with nitroimidazole reductase: a phase I and pharmacokinetic study of its prodrug, CB1954. Clin Cancer Res 2001;7:2662–8.
7. Patel P, Young JG, Mautner V, Ashdown D, Bonney S, Pineda RG, et al. A phase I/II clinical trial in localized prostate cancer of an adenovirus expressing nitroreductase with CB1954 [correction of CB1984]. Mol Ther 2009;1:1292–9.
8. Rainov NG. A phase III clinical evaluation of herpes simplex virus type 1 thymidine kinase and ganciclovir gene therapy as an adjuvant to surgical resection and radiation in adults with previously untreated glioblastoma multiforme. Hum Gene Ther 2000;11:2389–401.
9. Thery C, Witwer KW, Aikawa E, Alcaraz MJ, Anderson JD, Andriantsitohaina R, et al. Minimal information for studies of extracellular vesicles 2018 (MISEV2018): a position statement of the International Society for Extracellular Vesicles and update of the MISEV2014 guidelines. J Extracell Vesicles 2018;7:1535750.
10. Zhu X, Badawi M, Pomeroy S, Sutaria DS, Xie Z, Baek A, et al. Comprehensive toxicity and immunogenicity studies reveal minimal effects in mice following sustained dosing of extracellular vesicles derived from HEK293T cells. J Extracell Vesicles 2017;6:1324730.
11. Takahashi A, Okada R, Nagao K, Kawamata Y, Hanyu A, Yoshimoto S, et al. Exosomes maintain cellular homeostasis by excreting harmful DNA from cells. Nat Commun 2017;8:15287.
12. Delcayre A, Le Pecq JB. Exosomes as novel therapeutic nanodevices. Curr Opin Mol Ther 2006;8:31–8.
13. Mentkowski KI, Snitzer JD, Rusnak S, Lang JK. Therapeutic potential of engineered extracellular vesicles. AAPS J 2018;20:50.
14. Zou S, Scarfo K, Nantz MH, Hecker JG. Lipid-mediated delivery of RNA is more efficient than delivery of DNA in non-dividing cells. Int J Pharm 2010;389:232–43.
15. Marx V. How to pull the blanket off dormant cancer cells. Nat Methods 2018;15:249–52.

16. Okumura K, Nakase M, Inui M, Nakamura S, Watanabe Y, Tagawa T. Bax mRNA therapy using cationic liposomes for human malignant melanoma. J Gene Med 2008;10:910–7.
17. Thorne SH, Barak Y, Liang W, Bachmann MH, Rao J, Contag CH, et al. CNOB/ChrR6, a new prodrug enzyme cancer chemotherapy. Mol Cancer Ther 2009;8:333–41.
18. Wang JH, Endsley AN, Green CE, Matin AC. Utilizing native fluorescence imaging, modeling and simulation to examine pharmacokinetics and therapeutic regimen of a novel anticancer prodrug. BMC Cancer 2016;16:524.
19. Kanada M, Bachmann MH, Hardy JW, Frimannson DO, Bronsart L, Wang A, et al. Differential fates of biomolecules delivered to target cells via extracellular vesicles. Proc Natl Acad Sci U S A 2015;112:E1433–42.
20. Bolukbasi MF, Mizrak A, Ozdener GB, Madlener S, Strobel T, Erkan EP, et al. miR-1289 and "Zipcode"-like Sequence Enrich mRNAs in Microvesicles. Mol Ther Nucleic Acids 2012;1:e10.
21. Barak Y, Nov Y, Ackerley DF, Matin A. Enzyme improvement in the absence of structural knowledge: a novel statistical approach. ISME J 2008;2:171–9.
22. Barak Y, Thorne SH, Ackerley DF, Lynch SV, Contag CH, Matin A. New enzyme for reductive cancer chemotherapy, YieF, and its improvement by directed evolution. Mol Cancer Ther 2006;5:97–103.
23. Phua KK, Leong KW, Nair SK. Transfection efficiency and transgene expression kinetics of mRNA delivered in naked and nanoparticle format. J Control Release 2013;166:227–33.
24. Poliskey JA, Crowley ST, Ramanathan R, White CW, Mathew B, Rice KG. Metabolically stabilized double-stranded mRNA polyplexes. Gene Ther 2018;25:473–84.
25. Lehouritis P, Stanton M, McCarthy FO, Jeavons M, Tangney M. Activation of multiple chemotherapeutic prodrugs by the natural enzymolome of tumour-localised probiotic bacteria. J Control Release 2016;222:9–17.
26. Imai T, Takahashi Y, Nishikawa M, Kato K, Morishita M, Yamashita T, et al. Macrophage-dependent clearance of systemically administered B16BL6-derived exosomes from the blood circulation in mice. J Extracell Vesicles 2015;4:26238.
27. Lai CP, Mardini O, Ericsson M, Prabhakar S, Maguire C, Chen JW, et al. Dynamic biodistribution of extracellular vesicles in vivo using a multimodal imaging reporter. ACS Nano 2014;8:483–94.
28. Tang MH, Helsby NA, Goldthorpe MA, Thompson KM, Al-Ali S, Tingle MD. Hepatic nitroreduction, toxicity and toxicokinetics of the anti-tumour prodrug CB 1954 in mouse and rat. Toxicology 2007;240:70–85.
29. Li X, Stuckert P, Bosch I, Marks JD, Marasco WA. Single-chain antibody-mediated gene delivery into ErbB2-positive human breast cancer cells. Cancer Gene Ther 2001;8:555–65.
30. Rudnick SI, Lou J, Shaller CC, Tang Y, Klein-Szanto AJ, Weiner LM, et al. Influence of affinity and antigen internalization on the uptake and penetration of Anti-HER2 antibodies in solid tumors. Cancer Res 2011;71:2250–9.
31. Black ME, Kokoris MS, Sabo P. Herpes simplex virus-1 thymidine kinase mutants created by semi-random sequence mutagenesis improve prodrug-mediated tumor cell killing. Cancer Res 2001;61:3022–6.
32. Helsby NA, Atwell GJ, Yang S, Palmer BD, Anderson RF, Pullen SM, et al. Aziridinyldinitrobenzamides: synthesis and structure-activity relationships for activation by E. coli nitroreductase. J Med Chem 2004;47:3295–307.
33. Eswaramoorthy S, Poulain S, Hienerwadel R, Bremond N, Sylvester MD, Zhang YB, et al. Crystal structure of ChrR–a quinone reductase with the capacity to reduce chromate. PLoS One 2012;7:e36017.
34. Helsby NA, Ferry DM, Patterson AV, Pullen SM, Wilson WR. 2-Amino metabolites are key mediators of CB 1954 and SN 23862 bystander effects in nitroreductase GDEPT. Br J Cancer 2004;90:1084–92.
35. Schepelmann S, Spooner R, Friedlos F, Marais R. Methods to improve efficacy in suicide gene therapy approaches: targeting prodrug-activating enzymes carboxypeptidase G2 and nitroreductase to different subcellular compartments. Methods Mol Med 2004;90:279–301.
36. Ohno S, Takanashi M, Sudo K, Ueda S, Ishikawa A, Matsuyama N, et al. Systemically injected exosomes targeted to EGFR deliver antitumor microRNA to breast cancer cells. Mol Ther 2013;21:185–91.
37. Wahlgren J, Karlson TD, Brisslert M, Vaziri Sani F, Telemo E, Sunnerhagen P, et al. Plasma exosomes can deliver exogenous short interfering RNA to monocytes and lymphocytes. Nucleic Acids Res 2012;40:e130.
38. Liu Y, Li D, Liu Z, Zhou Y, Chu D, Li X, et al. Targeted exosome-mediated delivery of opioid receptor Mu siRNA for the treatment of morphine relapse. Sci Rep 2015;5:17543.
39. Liang G, Kan S, Zhu Y, Feng S, Feng W, Gao S. Engineered exosome-mediated delivery of functionally active miR-26a and its enhanced suppression effect in HepG2 cells. Int J Nanomedicine 2018;13:585–99.
40. Kao SC, Fulham M, Wong K, Cooper W, Brahmbhatt H, MacDiarmid J, et al. A Significant metabolic and radiological response after a novel targeted MicroRNA-based treatment approach in malignant pleural mesothelioma. Am J Respir Crit Care Med 2015;191:1467–9.
41. Kanada M, Kim BD, Hardy JW, Ronald JA, Bachmann MH, Bernard MP, et al. Microvesicle-mediated delivery of minicircle DNA results in effective gene-directed enzyme prodrug cancer therapy. Mol Cancer Ther 2019;18:2331–42.
42. Kojima R, Bojar D, Rizzi G, Hamri GC, El-Baba MD, Saxena P, et al. Designer exosomes produced by implanted cells intracerebrally deliver therapeutic cargo for Parkinson's disease treatment. Nat Commun 2018;9:1305.
43. Hung ME, Leonard JN. A platform for actively loading cargo RNA to elucidate limiting steps in EV-mediated delivery. J Extracell Vesicles 2016;5:31027.
44. Kasperzyk JL, Finn SP, Flavin R, Fiorentino M, Lis R, Hendrickson WK, et al. Prostate-specific membrane antigen protein expression in tumor tissue and risk of lethal prostate cancer. Cancer Epidemiol Biomarkers Prev 2013;22:2354–63.
45. Lu Y, Low PS. Immunotherapy of folate receptor-expressing tumors: review of recent advances and future prospects. J Control Release 2003;91:17–29.
46. Reynolds AR, Moein Moghimi S, Hodivala-Dilke K. Nanoparticle-mediated gene delivery to tumour neovasculature. Trends Mol Med 2003;9:2–4.
47. Boczkowski D, Nair SK, Nam JH, Lyerly HK, Gilboa E. Induction of tumor immunity and cytotoxic T lymphocyte responses using dendritic cells transfected with messenger RNA amplified from tumor cells. Cancer Res 2000;60:1028–34.
48. Phua KK, Boczkowski D, Dannull J, Pruitt S, Leong KW, Nair SK. Whole blood cells loaded with messenger RNA as an anti-tumor vaccine. Adv Healthc Mater 2014;3:837–42.
49. Milani A, Sangiolo D, Aglietta M, Valabrega G. Recent advances in the development of breast cancer vaccines. Breast Cancer 2014;6:159–68.
50. Turpin J, Ling C, Crosby EJ, Hartman ZC, Simond AM, Chodosh LA, et al. The ErbB2DeltaEx16 splice variant is a major oncogenic driver in breast cancer that promotes a pro-metastatic tumor microenvironment. Oncogene 2016;35:6053–64.
51. Weissman D, Ni H, Scales D, Dude A, Capodici J, McGibney K, et al. HIV gag mRNA transfection of dendritic cells (DC) delivers encoded antigen to MHC Class I and II molecules, Causes DC maturation, and induces a potent human in vitro primary immune response. J Immunol 2000;165:4710–7.
52. Russell JE, Liebhaber SA. The stability of human beta-globin mRNA is dependent on structural determinants positioned within its 3′ untranslated region. Blood 1996;87:5314–23.
53. Steinle H, Behring A, Schlensak C, Wendel HP, Avci-Adali M. Concise review: application of *in vitro* transcribed messenger RNA for cellular engineering and reprogramming: progress and challenges. Stem Cells 2017;35:68–79.
54. Cheng C, Convertine AJ, Stayton PS, Bryers JD. Multifunctional triblock copolymers for intracellular messenger RNA delivery. Biomaterials 2012;33:6868–76.
55. Gallie DR. Cap-independent translation conferred by the 5′ leader of tobacco etch virus is eukaryotic initiation factor 4G dependent. J Virol 2001;75:12141–52.
56. Khan MA, Yumak H, Goss DJ. Kinetic mechanism for the binding of eIF4F and tobacco Etch virus internal ribosome entry site RNA: effects of eIF4B and poly (A)-binding protein. J Biol Chem 2009;284:35461–70.

Published OnlineFirst January 15, 2020; DOI: 10.1158/1535-7163.MCT-19-0928

Molecular Cancer Therapeutics

Extracellular Vesicle–Mediated *In Vitro* Transcribed mRNA Delivery for Treatment of HER2 $^{+}$ Breast Cancer Xenografts in Mice by Prodrug CB1954 without General Toxicity

Alexis V. Forterre, Jing-Hung Wang, Alain Delcayre, et al.

Mol Cancer Ther 2020;19:858-867. Published OnlineFirst January 15, 2020.